Shikha Deep[1*], *Sandeep Kumar Paul*[2]

AN ANALYTICAL APPROACH FOR LOVE WAVE DISPERSION IN A VISCOELASTIC LAYER LYING ON AN ELASTIC LAYER WITH IMPERFECT INTERFACE: UNDER STRESS-FREE AND CLAMPED BOUNDARY CONDITIONS

ANALITIČKI PRISTUP DISPERZIJI LOVE TALASA U VISKOELASTIČNOM SLOJU NAD ELASTIČNIM SLOJEM SA NESAVRŠENIM INTERFEJSOM: U USLOVIMA BEZ NAPONA I PRI GRANIČNIM USLOVIMA UKLJEŠTENJA

Originalni naučni rad / Original scientific paper
Rad primljen / Paper received: 15.07.2024
https://doi.org/10.69644/ivk-2025-siA-0035

Adresa autora / Author's address:
[1)] United World Institute of Technology, Karnavati University, Gandhinagar, Gujarat, India *email: shikhathakur493@gmail.com
[2)] Department of Mathematics, School of Chemical Engineering and Physical Sciences, Lovely Professional University, Phagwara, Punjab, India

Keywords

- Love waves
- viscoelastic materials
- isotropic medium
- imperfect interface
- clamped layer

Ključne reči

- Love talasi
- viskoelastični materijali
- izotropna sredina
- nesavršen interfejs
- uklješteni sloj

Aopbstract

The problem is investigated on the propagation of Love type waves in a geometrical configuration composed of an inhomogeneous viscoelastic layer lying over an elastic substrate. The viscoelastic layer and an isotropic substrate are imperfectly attached to each other. An analysis is done in two cases, first, when the top surface of viscoelastic layer is stress-free, and second, when it is clamped. The dispersion and damping relations for both stress-free and clamped cases are separately determined through the use of effective boundary conditions. A special case is also derived when the viscoelastic layer is perfectly attached to the substrate under both conditions. An analytical approach is performed, and results are drawn graphically to explore the impacts of various parameters such as heterogeneity, internal friction, thickness of the layer and imperfectness parameter in both cases on phase and damping velocities of Love waves.

Izvod

Problem se tretira istraživanjem prostiranja Love talasa u geometrijskog konfiguraciji sačinjenoj iz nehomogenog viskoelastičnog sloja koji leži iznad elastičnog supstrata. Viskoelastičan sloj i izotropni supstrat su nesavršeno povezani. Analiza je urađena za dva slučaja. U prvom je gornji viskoelastični sloj bez napona, a u drugom je vezan (uklješten). Relacije koje opisuju disperziju i prigušenje za oba slučaja, bez napona i sa uklještenjem, se određuju nezavisno, putem uticajnih graničnih uslova. Razmotren je i specijalan slučaj, kada je viskoelastičan sloj idealno vezan sa supstratom, za oba navedena slučaja. Analitičkim pristupom se dobijaju rezultati koji su predstavljeni grafički, čime se pokazuje uticaj raznih parametara, na pr. heterogenosti, unutrašnjeg trenja, debljine sloja i parametra nesavršenosti veze na fazne i brzine prigušenja Love talasa, kod oba spomenuta slučaja.

INTRODUCTION

Theoretical examination of seismic waves is an essential instrument for investigating the complex interior of the Earth with accuracy, comprehending earthquakes, and devising efficient strategies to alleviate their impacts. During earthquakes and explosions, many types of waves are detected, and Love waves are one of them. Love waves are surface waves characterised by horizontal particle motion solely along the surface of the medium and normal to the direction of wave propagation. These waves travel through a stratified configuration, consisting of a layer having finite thickness succeeded by a substrate. For the origination of these waves, the surface layer needs to be slower than the substrate. Numerous researchers have delved into these types of waves analysing diverse geometric configurations, employing a range of parameters, and utilising distinct mechanical theories /1-7/. The displacement attributes of Love waves are readily understandable as they propagate with a single displacement component, rendering them highly suitable for applications as guided waves in non-destructive evaluation methodologies, structural health monitoring, and signal processing equipment. Love type waves are utilised in SAW devices as SH/Love waves sensors, contributing to non-destructive evaluation techniques for material characterisation. Additionally, these waves serve as SH/Love wave biosensors to detect diseases within the human body, /8-12/.

The interior of the Earth exhibits inhomogeneity due to many factors. These factors must be considered in mathematical formulations when conducting theoretical investigations on wave propagation within an Earth-like infinite geometrical configuration. The heterogeneity of the medium can be incorporated into mathematical models by introducing a depth-dependent heterogeneity parameter utilising various mathematical functions like linear, quadratic, exponential, trigonometric functions, and more. Several researchers have investigated the influence of material heterogeneity on the behaviour of different wave types propagating in varied geometric setups through the application of diverse mechanical theories, /13-17/.

The study of seismic waves in layered media is crucial for understanding seismic behaviour in complex environments. Investigating the mechanical behaviour of viscoelastic media is particularly important because the asthenosphere, a transition zone between the low-density crust and higher-density mantle, is viscous. Most dynamic Earth processes responsible for earthquakes occur in this zone, leading to various physical phenomena. The Earth, composed of silicate and iron-alloy materials, responds nearly elastically to small-magnitude transient forces but behave viscously under long-duration forces across the range of pressures and temperatures within the planet. Subsurface materials like coal tar, salt, and sediments can be modelled as viscoelastic materials which are considered in the broader context of their physical properties. Materials used in structural and engineering applications may exhibit viscoelastic behaviour, significantly impacting their performance. In some cases, viscoelasticity is intentionally utilised in the design process to achieve specific objectives. Many researchers have studied the types of wave propagation in different variations in the density and rigidity of the viscoelastic medium, /18-22/.

Various layers inside the Earth are not perfectly bonded, and these imperfections can affect wave propagation. Additionally, the Earth's crust comprises layers of different materials that are not in perfect contact. Imperfections at the interface between two materials can arise from faulty manufacturing processes, accumulated damage, and thermal mismatch. In a perfect contact condition, stress and displacement components are continuous across the interface. However, in the case of an imperfect interface, while stress components remain continuous, the displacement components are discontinuous, with the displacement jump being proportional to the stress vector. Numerous authors have incorporated the concept of imperfections at interfacial surfaces in various models for wave propagation problems, /23-27/.

Kaplunov et al. /28/ investigated the propagation of Love waves in a layered structure with a clamped surface. According to their findings, Love waves can exist in a clamped layered structure if the shear wave velocity of the half-space exceeds the velocity of layer. While Love waves have been extensively analysed by numerous researchers in a stress-free layered structure, the literature pertaining to Love waves in a clamped layered structure appears to be limited based on the findings of previous researchers. Some researchers investigated the propagation of waves by using the conditions of clamped surface, /29, 30/.

Love wave propagation is extensively studied in various layered structures with different material compositions and boundary conditions. The present problem studies propagation of Love waves in two scenarios, one when the top surface of layer is stress-free and the other, in which upper surface of layer is clamped. Under the effective boundary conditions dispersion and damping equations are obtained. This problem explores the impact of various parameters like heterogeneity, internal friction, thickness of the layer and imperfectness parameter on phase and damping velocities of Love waves in both stress-free and clamped conditions at the top surface of the layer.

FORMULATION OF THE PROBLEM

For this study, a viscoelastic layer of finite and uniform thickness (H) is imperfectly attached to an elastic substrate as depicted in Fig. 1. The origin of co-ordinate system (x,y,z) is considered at the joining interface of two media. It is assumed that the wave is propagating along the direction of x-axis and z-axis is positive going downwards into the substrate. The displacement components for the layer are (u_1, v_1, w_1) and for the elastic substrate as (u_2, v_2, w_2). The field variables are assumed to be not dependent upon y-axis, that is $\partial/\partial y \equiv 0$. The Love waves will propagate with only single non-zero displacement component, so as per the geometry of the problem, it is assumed $u_1 = w_1 = 0$, $u_2 = w_2 = 0$, $v_1 = v_1(x,z,t)$ and $v_2(x,z,t)$.

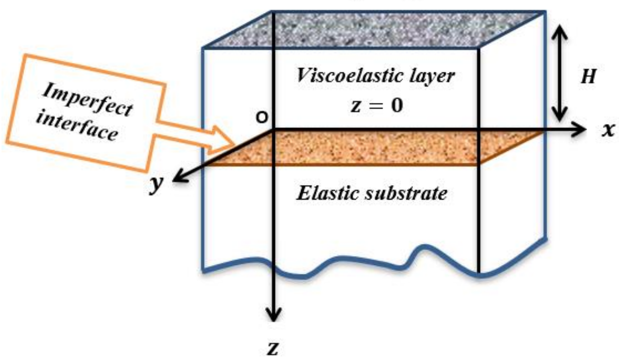

Figure 1. Geometry of the problem.

SOLUTION OF THE PROBLEM

Heterogeneous viscoelastic layer

The equation of motion for the heterogeneous viscoelastic layer can be written as, /31/,

$$\left(\frac{\partial \tau_{xy}}{\partial x} + \frac{\partial \tau_{yz}}{\partial z}\right) = \rho_1 \frac{\partial^2 v_1}{\partial t^2}\,, \tag{1}$$

where: ρ_1 is the density of material.

The constitutive relation for viscoelastic medium is

$$\tau_{ij} = \left(\lambda_1 + \lambda_1' \frac{\partial}{\partial t}\right)\delta_{ij} v_{k,k} + \left(\mu_1 + \eta_1 \frac{\partial}{\partial t}\right)(v_{i,j} + v_{j,i})\,, \tag{2}$$

where: μ_1 and λ_1 are Lame's constants; λ_1' and η_1 are internal friction parameters; τ_{ij} are stress components; δ_{ij} is Kronecker's delta; and v_i are the displacement components for viscoelastic layer; i, j, k = 1, 2, 3.

Due to the presence of heterogeneity in the viscoelastic layer, μ_1, η_1, and ρ_1 are taken as the function of depth only and are given by

$$\begin{aligned} \mu_1 &= \mu_0(1-\sin\alpha z)\,, \\ \eta_1 &= \eta_0(1-\sin\alpha z)\,, \\ \rho_1 &= \rho_0(1-\sin\alpha z)\,, \end{aligned} \tag{3}$$

where: μ_0, η_0, ρ_0 are the constant values of μ_1, η_1, and ρ_1. Here, α is an arbitrary constant having dimensions of inverse length.

The non-vanishing stress components

$$\tau_{xy} = \left(\mu_1 + \eta_1 \frac{\partial}{\partial t}\right)\frac{\partial v_1}{\partial x} = \tau_{yx} \text{ and } \tau_{yz} = \left(\mu_1 + \eta_1 \frac{\partial}{\partial t}\right)\frac{\partial v_1}{\partial z} = \tau_{zy}\,. \tag{4}$$

Using Eq.(3) and Eq.(4) in Eq.(1), we get

$$\left(\mu_1+\eta_1\frac{\partial}{\partial t}\right)\frac{\partial^2 v_1}{\partial x^2}+\frac{\partial}{\partial z}\left[\left(\mu_1+\eta_1\frac{\partial}{\partial t}\right)\frac{\partial v_1}{\partial z}\right]=\rho_1\frac{\partial^2 v_1}{\partial t^2}. \quad (5)$$

After assuming the solution for Eq.(5) as $v_1 = g(z)e^{-i(\omega t-kx)}$, where k is wave number, $\omega = kc$ is angular frequency and c is phase velocity, we get the following differential equation

$$\frac{d^2 g}{dz^2}+\frac{(\bar{\mu}_1)'}{\bar{\mu}_1}\frac{dg}{dz}+\left(\frac{\rho_1\omega^2}{\bar{\mu}_1}-k^2\right)g(z)=0, \quad (6)$$

where: $\bar{\mu}_1 = \mu_1 - i\omega\eta_1$; and $(\bar{\mu}_1) = d\bar{\mu}_1/dz = \partial\mu_1/\partial z - i\omega(\partial\eta_1/\partial z)$.

Taking $g(z) = Y_1(z)/\sqrt{\bar{\mu}_1}$, Eq.(6) reduces to

$$\frac{d^2Y_1}{dz^2}+\left[\frac{1}{4(\bar{\mu}_1)^2}\left(\frac{d\bar{\mu}_1}{dz}\right)^2-\frac{1}{2\bar{\mu}_1}\frac{d^2\bar{\mu}_1}{dz^2}+\frac{\rho_1\omega^2}{\bar{\mu}_1}-k^2\right]Y_1=0, \quad (7)$$

Solving Eq.(7) further, gives

$$\frac{d^2Y_1}{dz^2}-m^2Y_1=0, \quad (8)$$

where: $m^2 = k^2 - (a^2/4) - (\rho_0\omega^2/\bar{\mu}_1)$; and $\bar{\mu}_1 = \mu_0 - i\omega\eta_0$.

The solution of the above differential equation Eq.(8) becomes

$$Y_1(z)=A_1e^{t_1 z}+B_1e^{-t_1 z}. \quad (9)$$

Therefore, the displacement component of the upper viscoelastic layer becomes

$$v_1(x,z,t)=\frac{A_1e^{t_1 z}+B_1e^{-t_1 z}}{\sqrt{\bar{\mu}_0}\sqrt{1-\sin\alpha z}}e^{-i(\omega t-kx)}, \quad (10)$$

and we get the stress component as

$$\tau_{yz}=\frac{\sqrt{\bar{\mu}_0}}{2\sqrt{1-\sin\alpha z}}\left\{\left[\alpha\cos\alpha z+2t_1(1-\sin\alpha z)\right]e^{t_1 z}A_1+\right.$$
$$\left.\left[\alpha\cos\alpha z-2t_1(1-\sin\alpha z)\right]e^{-t_1 z}B_1\right\}e^{-i(\omega t-kx)}, \quad (11)$$

where: t_1 is given in Appendix 1.

Isotropic elastic substrate

The equation of motion for homogeneous isotropic elastic medium are given as

$$\frac{\partial\sigma_{xx}}{\partial x}+\frac{\partial\sigma_{xy}}{\partial y}+\frac{\partial\sigma_{xz}}{\partial z}=\rho_2\frac{\partial^2u_2}{\partial t^2},$$
$$\frac{\partial\sigma_{yx}}{\partial x}+\frac{\partial\sigma_{yy}}{\partial y}+\frac{\partial\sigma_{yz}}{\partial z}=\rho_2\frac{\partial^2v_2}{\partial t^2}, \quad (12)$$
$$\frac{\partial\sigma_{zx}}{\partial x}+\frac{\partial\sigma_{zy}}{\partial y}+\frac{\partial\sigma_{zz}}{\partial z}=\rho_2\frac{\partial^2w_2}{\partial t^2}.$$

The stress - strain relationship for an isotropic medium is

$$\sigma_{ij}=\lambda_2\Delta\delta_{ij}+2\mu_2e_{ij}, \quad (13)$$

where: σ_{ij} are stress components; λ_2 and μ_2 are Lame's constants; ρ_2 is density of material; $e_{ij} = [(\partial u_i/\partial x_j)+(\partial u_j/\partial x_i)]/2$ are strain components; $\Delta = e_{11} + e_{22} + e_{33}$ is volumetric strain; and δ_{ij} is Kronecker's delta; $i, j = 1, 2, 3$.

Using mentioned conditions for the propagation of Love waves, the non-vanishing stress components are

$$\sigma_{xy}=\mu_2\frac{\partial v_2}{\partial x}=\sigma_{yx} \text{ and } \sigma_{yz}=\mu_2\frac{\partial v_2}{\partial z}=\sigma_{zy}. \quad (14)$$

The only non-vanishing equation of motion from Eq.(12) is given as

$$\frac{\partial^2v_2}{\partial x^2}+\frac{\partial^2v_2}{\partial z^2}=\frac{1}{\beta_2^2}\frac{\partial^2v_2}{\partial t^2}, \quad (15)$$

where: $\beta_2^2 = \mu_2/\rho_2$.

Assume the solution of Eq.(15) as $v_2(x,z,t) = h(z)e^{-i(\omega t-kx)}$, where k is wave number, $\omega = kc$ is angular frequency, and c is phase velocity, we get the following differential equation

$$\frac{d^2h}{dz^2}-P^2k^2h(z)=0. \quad (16)$$

The solution of differential equation in Eq.(16) becomes

$$h(z)=A_2e^{kPz}+B_2e^{-kPz}. \quad (17)$$

As $z \to \infty$, $h(z)$ must vanish, so to make this happen, we take $A_2 = 0$, hence, the solution given in Eq.(17) becomes $h(z) = B_2e^{-kPz}$.

Hence, the displacement component for an isotropic elastic substrate is

$$v_2(x,z,t)=B_2e^{-kPz}e^{-i(\omega t-kx)}, \quad (18)$$

where: $P = \sqrt{(1 - c^2/\beta_2^2)}$, and we get the stress component as

$$\sigma_{yz}=\mu_2B_2e^{-kPz}(-kP)e^{-i(\omega t-kx)}. \quad (19)$$

BOUNDARY CONDITIONS

Stress-free boundary conditions

i. The stress component vanishes at the upper surface of layer, that is $\tau_{yz} = 0$ at $z = -H$.
ii. Layer and substrate are not perfectly attached, so the difference in displacement components is proportional to stress tensor, that is $\tau_{yz} = G(v_2 - v_1)$ at $z = 0$, where G defines the degree of imperfectness.
iii. Stress components are continuous at the joining interface, so, $\tau_{yz} = \sigma_{yz}$ at $z = 0$.

By implementing the above-mentioned boundary conditions, we obtain following equations

$$\sqrt{\bar{\mu}_0}[\alpha\cos\alpha H+2t_1(1+\sin\alpha H)]e^{-t_1H}A_1+$$
$$+\sqrt{\bar{\mu}_0}[\alpha\cos\alpha H-2t_1(1+\sin\alpha H)]e^{-t_1H}B_1=0, \quad (20)$$

$$\left[\frac{(\alpha+2t_1)\sqrt{\bar{\mu}_0}}{2}+\frac{G}{\sqrt{\bar{\mu}_0}}\right]A_1+\left[\frac{(\alpha-2t_1)\sqrt{\bar{\mu}_0}}{2}+\frac{G}{\sqrt{\bar{\mu}_0}}\right]B_1-GB_2=0 \quad (21)$$

$$\left[\frac{(\alpha+2t_1)\sqrt{\bar{\mu}_0}}{2}\right]A_1+\left[\frac{(\alpha-2t_1)\sqrt{\bar{\mu}_0}}{2}\right]B_1+(\mu_2kP)B_2=0. \quad (22)$$

For the non-trivial solution of Eqs.(20)-(22), determinant of the arbitrary coefficients must vanish. After solving the determinant, the following equation is obtained for the propagation of Love waves in the considered geometry, under stress-free conditions at top surface of layer, when this layer and the substrate are imperfectly attached,

$$[W_1e^{-m_1'H}+W_2e^{-m_1'H}\tan(m_2'H)-W_3e^{m_1'H}+W_4e^{m_1'H}\tan(m_2'H)]+$$
$$+i[W_2e^{-m_1'H}-W_1e^{-m_1'H}\tan(m_2'H)-W_4e^{m_1'H}-$$
$$-W_3e^{m_1'H}\tan(m_2'H)]=0. \quad (23)$$

From the real part of Eq.(23), the dispersion relation is

$$\tan(m_2'H)=\frac{W_3e^{m_1'H}-W_1e^{-m_1'H}}{W_4e^{m_1'H}+W_2e^{-m_1'H}}, \quad (24)$$

and from imaginary part of Eq.(23), the damping relation is given as

$$\tan(m_2'H)=\frac{-W_4e^{m_1'H}+W_2e^{-m_1'H}}{W_3e^{m_1'H}+W_1e^{-m_1'H}}. \quad (25)$$

Case 1: If $G \to \infty$, interface between viscoelastic layer and an isotropic elastic substrate becomes perfect in nature, then the following cases are concluded.

Sub case 1: The dispersion relation given in Eq.(24) reduces to

$$\tan(m_2' H) = \frac{W_3' e^{m_1' H} - W_1' e^{-m_1' H}}{W_4' e^{m_1' H} + W_2' e^{-m_1' H}} . \tag{26}$$

The Eq.(26) shows dispersion relation for propagation of Love waves under stress-free conditions when layer and half-space are perfectly attached.

Sub case 2: The damping relation given in Eq.(25), reduces to

$$\tan(m_2' H) = \frac{-W_4' e^{m_1' H} + W_2' e^{-m_1' H}}{W_3' e^{m_1' H} + W_1' e^{-m_1' H}} , \tag{27}$$

where: W_1, W_2, W_3, W_4, W_1', W_2', W_3', and W_4' are given in Appendix 2.

The Eq.(27) shows damping relation for propagation of Love waves under stress-free conditions when layer and half-space are perfectly attached.

Clamped boundary conditions

i. The displacement component must vanish at the upper surface of layer, that is $v_1(x,z,t) = 0$ at $z = -H$.
ii. Layer and substrate are not perfectly attached, so the difference in displacement components is proportional to stress tensor, that is $\tau_{yz} = G(v_2 - v_1)$ at $z = 0$, where G defines the degree of imperfectness.
iii. Stress components are continuous at the joining interface, so $\tau_{yz} = \sigma_{yz}$ at $z = 0$.

By implementing the above-mentioned boundary conditions, we obtain following equations

$$\frac{e^{-t_1 H}}{\sqrt{\bar{\mu}_0}} A_1 + \frac{e^{-t_1 H}}{\sqrt{\bar{\mu}_0}} B_1 = 0 , \tag{28}$$

$$\left(\frac{(\alpha + 2t_1)\sqrt{\bar{\mu}_0}}{2} + \frac{G}{\sqrt{\bar{\mu}_0}} \right) A_1 + \left(\frac{(\alpha - 2t_1)\sqrt{\bar{\mu}_0}}{2} + \frac{G}{\sqrt{\bar{\mu}_0}} \right) B_1 - -GB_2 = 0 , \tag{29}$$

$$\left(\frac{(\alpha + 2t_1)\sqrt{\bar{\mu}_0}}{2} \right) A_1 + \left(\frac{(\alpha - 2t_1)\sqrt{\bar{\mu}_0}}{2} \right) B_1 + (\mu_2 kP) B_2 = 0 . \tag{30}$$

For the non-trivial solution of Eqs.(28)-(30), determinant of arbitrary coefficients must vanish. After solving the determinant, the following equation is obtained for the propagation of Love waves in the considered geometry, under clamped conditions at top surface of layer, when layer and substrate are imperfectly attached,

$$[X_1 e^{-m_1' H} + X_2 e^{-m_1' H} \tan(m_2' H) - X_3 e^{m_1' H} + +X_4 e^{m_1' H} \tan(m_2' H)] + i[X_2 e^{-m_1' H} - X_1 e^{-m_1' H} \tan(m_2' H) - -X_4 e^{m_1' H} - X_3 e^{m_1' H} \tan(m_2' H)] = 0 . \tag{31}$$

From real part of Eq.(31), the dispersion relation is given as

$$\tan(m_2' H) = \frac{X_3 e^{m_1' H} - X_1 e^{-m_1' H}}{X_4 e^{m_1' H} + X_2 e^{-m_1' H}} , \tag{32}$$

and from imaginary part of Eq.(31), the damping relation is given as

$$\tan(m_2' H) = -\frac{X_4 e^{m_1' H} - X_2 e^{-m_1' H}}{X_3 e^{m_1' H} + X_1 e^{-m_1' H}} . \tag{33}$$

Case 2: If $G \to \infty$, the interface between heterogeneous viscoelastic layer and an isotropic elastic substrate becomes perfect in nature, then the following cases are concluded.

Sub case 1: The dispersion relation given in Eq.(32) reduces to

$$\tan(m_2' H) = \frac{X_3' e^{m_1' H} - X_1' e^{-m_1' H}}{X_4' e^{m_1' H} + X_2' e^{-m_1' H}} . \tag{34}$$

The Eq.(34) shows dispersion relation for propagation of Love waves under clamped conditions when layer and half-space are perfectly attached.

Sub case 2: The damping relation given in Eq.(33), reduces to

$$\tan(m_2' H) = -\frac{X_4' e^{m_1' H} - X_2' e^{-m_1' H}}{X_3' e^{m_1' H} + X_1' e^{-m_1' H}} , \tag{35}$$

where: X_1, X_2, X_3, X_4, X_1', X_2', X_3', and X_4' are given in Appendix 3.

The Eq.(35) shows damping relation for propagation of Love waves under clamped conditions when layer and half-space are perfectly attached.

NUMERICAL RESULTS AND DISCUSSION

The material constants taken for graphical illustrations are mentioned in Table 1.

Table 1. Material parameters.

Visco-elastic layer, /32/	$\mu_1 = 1.987 \cdot 10^{10}$ N/m^2	$\rho_1 = 4705$ kg/m^3	$\mu/\eta = 10^6$ s^{-1}
Elastic substrate	$\mu_2 = 7.10 \cdot 10^{10}$ N/m^2	$\rho_2 = 3321$ kg/m^3	–

Table 2. Values of various parameters.

Parameters	αH	μ_1/η_1	H	G
Figs. 2(a), (b) & 3(a), (b)	–	0.04	0.4	$30.5 \cdot 10^9$
Figs. 4(a), (b) & 5(a), (b)	0.1	–	0.4	$30.5 \cdot 10^9$
Figs. 6(a), (b) & 7(a), (b)	0.1	0.04	–	$30.5 \cdot 10^9$
Figs. 8(a), (b) & 9(a), (b)	0.1	0.04	0.4	–

Figures are plotted to represent the influence of heterogeneity parameter αH, internal friction parameter μ_1/η_1, thickness of layer H, and imperfectness parameter G, on the phase and damping velocities of Love waves, propagating in a viscoelastic layer which is imperfectly attached to an elastic substrate. In Figs. 2(a, b), 4(a, b), 6(a, b), and 8(a, b), results are plotted under stress-free conditions at the top surface of layer, and Figs. 3(a, b), 5(a, b), 7(a, b), and 9(a, b) are plotted under clamped conditions at top surface of the layer. Figures 2-7(a, b) are plotted when the viscoelastic layer is imperfectly attached to an isotropic elastic substrate. In the given figures, dimensionless phase-, or damping velocity c/β_1 is considered along y-axis, and dimensionless wave number kH is along x-axis.

Impacts of heterogeneity parameter αH

Figures 2(a, b) and 3(a, b) illustrate the changes in phase- or damping velocities caused by the impact of inhomogeneity parameter αH. The impact of heterogeneity parameter is exhibited through the consideration of three distinct values for inhomogeneity parameter as 0.18, 0.88, and 1.58. The values assigned to the remaining parameters are given in Table 2. It is evident that as the inhomogeneity parameter increases, there is a proportional rise in phase and damping velocities. In all the figures this trend indicates that the inhomogeneity parameter promotes phase and damping velocities within the medium for both stress-free and clamped conditions.

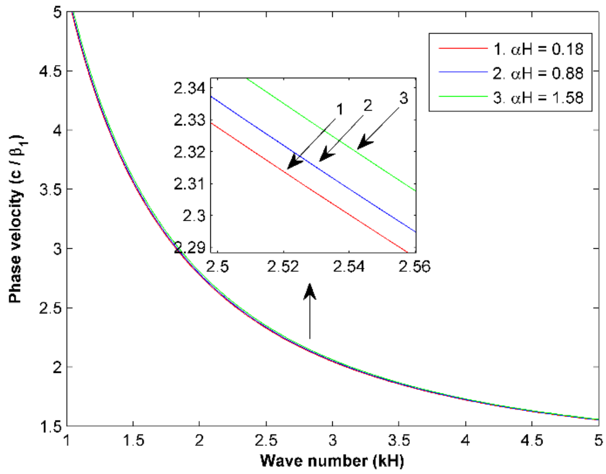

Figure 2a. Profiles of phase velocity c/β_1 of Love waves against wave number *kH* depicting impact of heterogeneity parameter αH under stress-free condition.

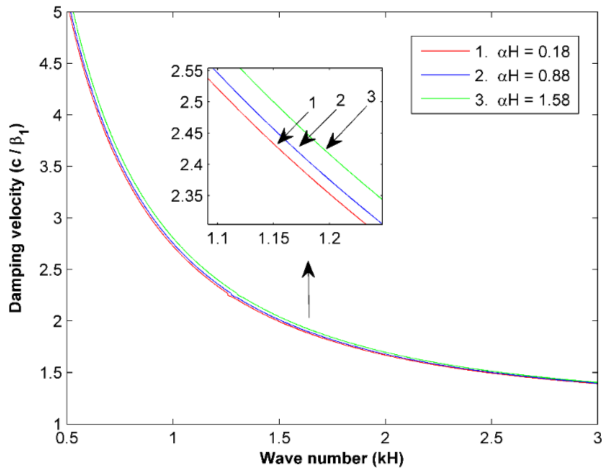

Figure 2b. Profiles of damping velocity c/β_1 of Love waves against wave number *kH* depicting impact of heterogeneity parameter αH under stress-free condition.

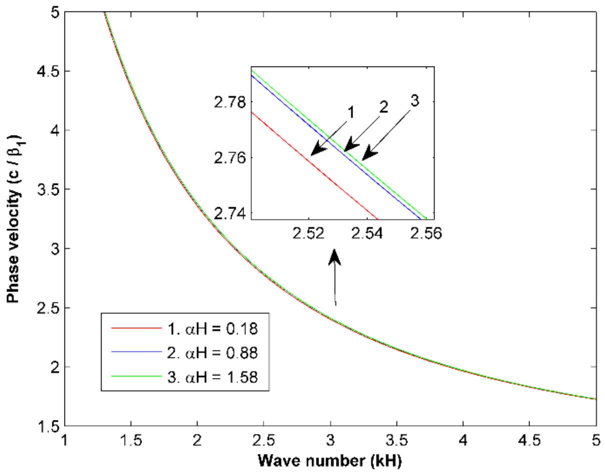

Figure 3a. Profiles of phase velocity c/β_1 of Love waves against wave number *kH* depicting impact of heterogeneity parameter αH under clamped condition.

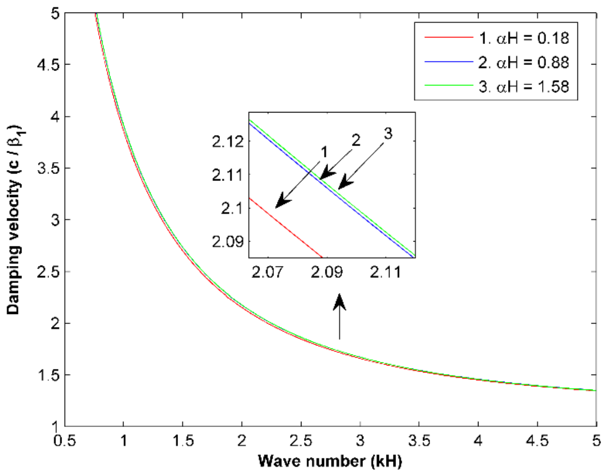

Figure 3b. Profiles of damping velocity c/β_1 of Love waves against wave number *kH* depicting impact of heterogeneity parameter αH under clamped condition.

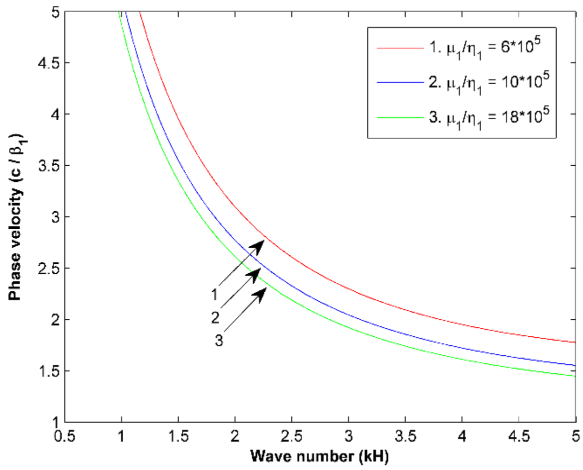

Figure 4a. Profiles of phase velocity c/β_1 of Love waves against wave number *kH* depicting impact of internal friction parameter μ_1/η_1 under stress-free condition.

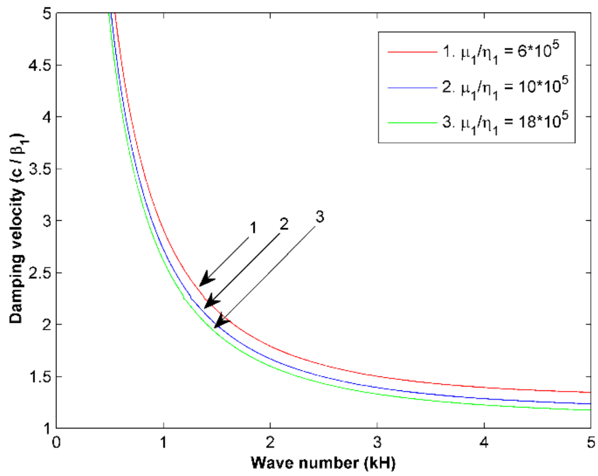

Figure 4b. Profiles of damping velocity c/β_1 of Love waves against wave number *kH* depicting impact of internal friction parameter μ_1/η_1 under stress-free condition

The impacts of internal friction parameter μ_1/η_1

The influence of the internal friction parameter μ_1/η_1 of the viscoelastic layer on the propagation of Love waves is demonstrated by using three different values of the parameter as 6×10^5, 10×10^5, and 18×10^5 in Figs. 4(a, b) and 5(a, b). The values assigned to the remaining parameters are given in Table 2. Examination of all figures reveals that an increase in internal friction parameter of the viscoelastic layer leads to a reduction in the phase- and damping velocities of Love waves under both stress-free and clamped conditions.

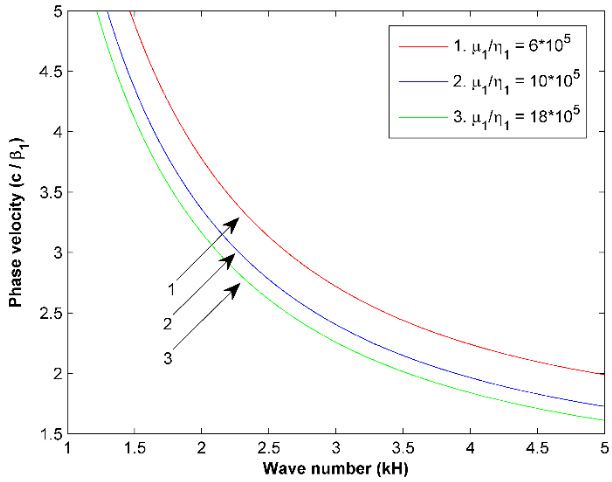

Figure 5a. Profiles of phase velocity c/β_1 of Love waves against wave number kH depicting impact of internal friction parameter μ_1/η_1 under clamped condition.

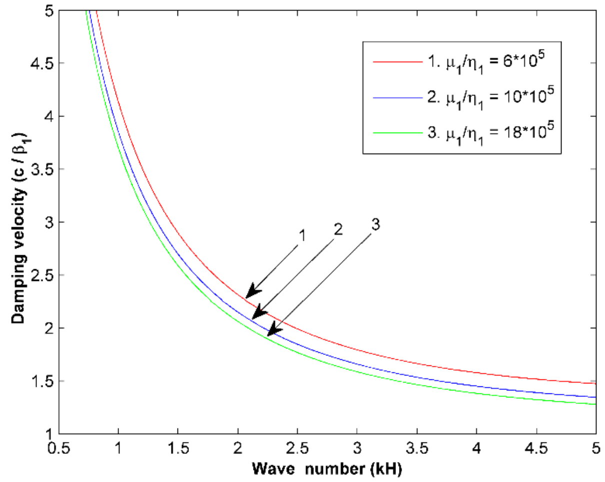

Figure 5b. Profiles of damping velocity c/β_1 of Love waves against wave number kH depicting impact of internal friction parameter μ_1/η_1 under clamped condition.

Impacts of thickness of the layer H

Figures 6(a, b) and 7(a, b) elucidate the influence of the thickness of layer H on the phase and damping velocities of Love waves. The values assigned to the remaining parameters are given in Table 2. For all figures, three distinct values of the thickness parameter are selected as 0.1 m, 0.2 m, and 0.3 m. Analysis of Figs. 6(a, b) and 7(a, b) reveal that the phase and damping velocities of Love waves decrease as the value of thickness parameter increases. It is observed that the results are the same under both stress-free and clamped conditions.

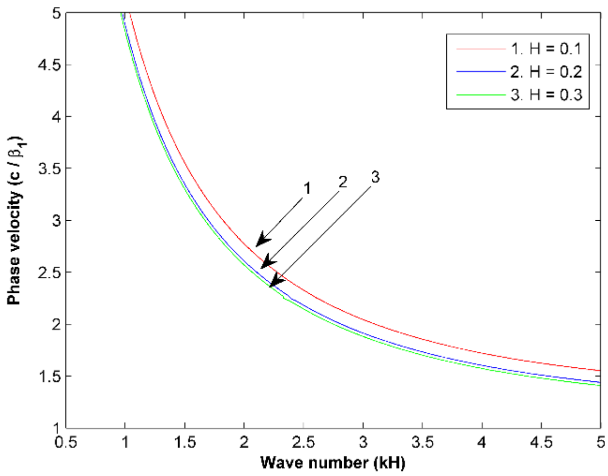

Figure 6a. Profiles of phase velocity c/β_1 of Love waves against wave number kH depicting impact of thickness of layer H under stress-free condition.

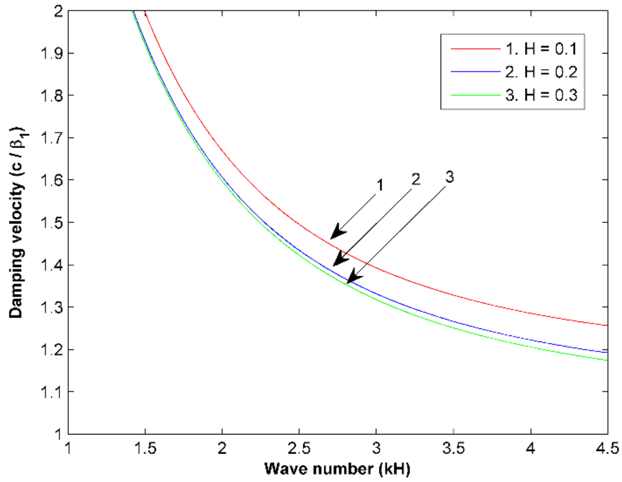

Figure 6b. Profiles of damping velocity c/β_1 of Love waves against wave number kH depicting impact of thickness of layer H under stress-free condition.

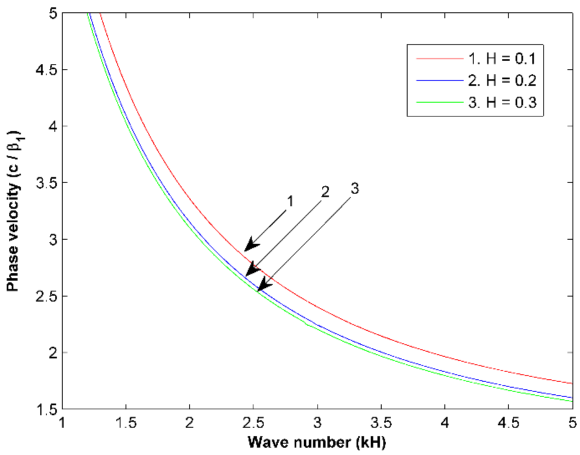

Figure 7a. Profiles of phase velocity c/β_1 of Love waves against wave number kH depicting impact of thickness of layer H under clamped condition.

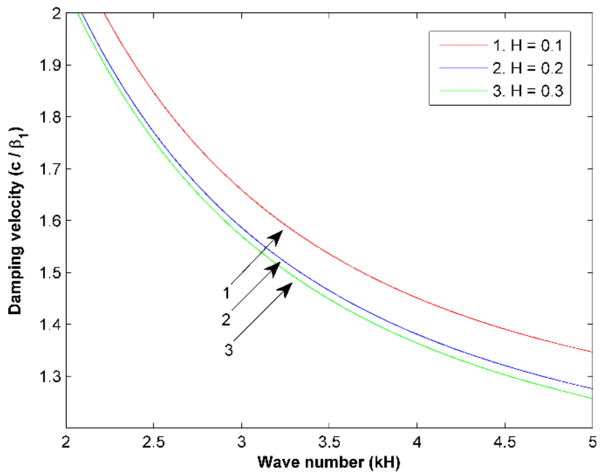

Figure 7b. Profiles of damping velocity c/β_1 of Love waves against wave number kH depicting impact of thickness of layer H under clamped condition.

Impacts of imperfectness parameter G

To determine the impact of imperfectness parameter G on propagation of Love waves, Figs. 8(a, b) and 9(a, b) are illustrated by using four values of $G = 1{*}30.5{\times}10^9$, $10{*}30.5{\times}10^9$, $20{*}30.5{\times}10^9$, and $G \to \infty$. The values assigned to remaining parameters are given in Table 2. When $G \to \infty$, it represents the heterogeneous viscoelastic layer and isotropic elastic substrate are perfectly attached to each other. Since the degree of imperfectness and the parameter G are inversely proportional, the trends indicate that as the degree of imperfectness decreases (i.e., G increases) at the interface, the phase and damping velocities increase. It can be also observed in all figures that the velocities are meeting at a particular point, and then again showing the same trend. From all figures, it can be examined that the phase and damping velocities are maximum when the two media are in perfect contact ($G \to \infty$).

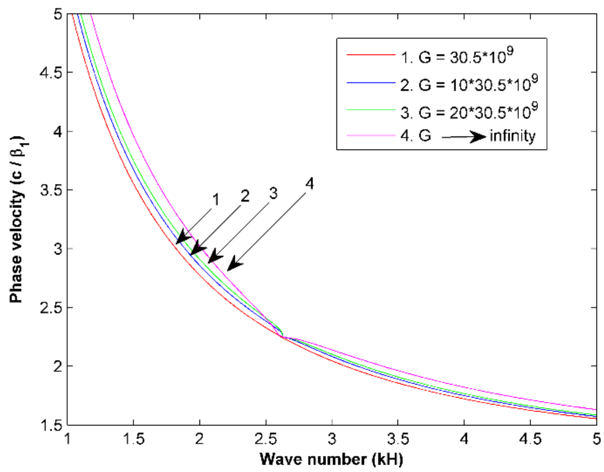

Figure 8a. Profiles of phase velocity c/β_1 of Love waves against wave number kH depicting impact of imperfectness parameter G under stress-free condition.

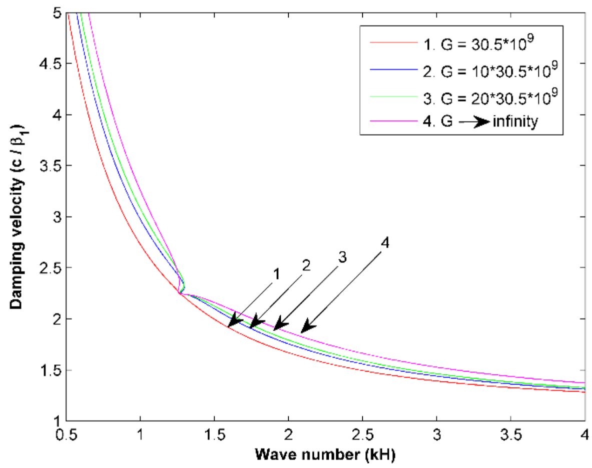

Figure 8b. Profiles of damping velocity c/β_1 of Love waves against wave number kH depicting impact of imperfectness parameter G under stress-free condition.

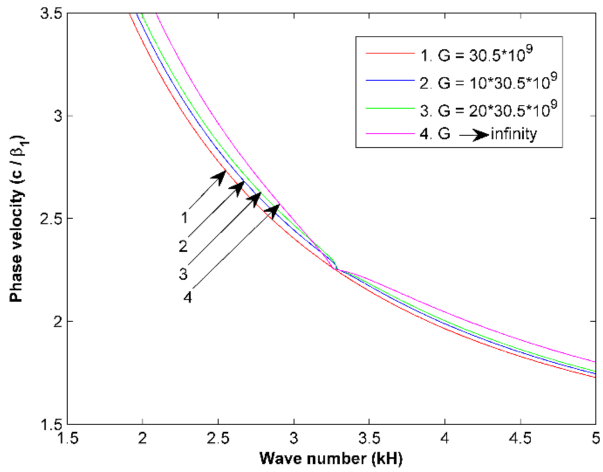

Figure 9a. Profiles of phase velocity c/β_1 of Love waves against wave number kH depicting impact of imperfectness parameter G under clamped condition.

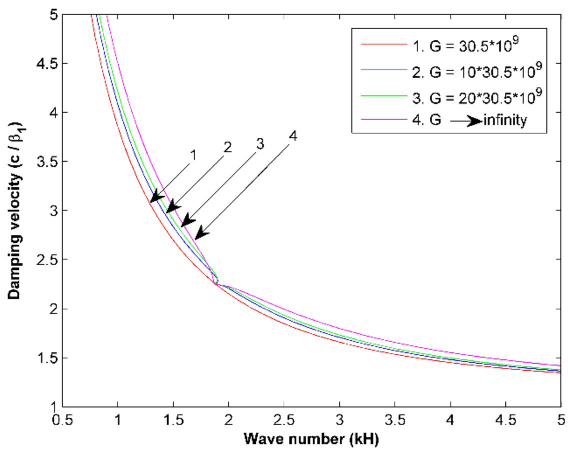

Figure 9b. Profiles of damping velocity c/β_1 of Love waves against wave number kH depicting impact of imperfectness parameter G under clamped condition.

CONCLUSIONS

A systematic investigation is conducted to analyse the dispersion and damping behaviour of Love waves in a heterogeneous viscoelastic layer that is imperfectly bonded to an isotropic elastic substrate under two distinct sets of boundary conditions. One scenario assumes the upper surface of the layer to be stress-free, while the other assumes the free surface of the layer to be clamped. It has been observed that the primary mode of Love waves lacks clarity; however, higher modes exhibit clear characteristics. Consequently, all graphical representations in this scenario are based on the first mode (n = 1) of Love waves. The study determines the effects of heterogeneity, internal friction, thickness of the layer and imperfectness parameter on the propagation of Love waves. The following major conclusions are derived from the results obtained.

i. The effects of the heterogeneity parameter of the viscoelastic layer on phase- and damping velocities of Love waves are illustrated. It is observed that the heterogeneity parameter favours phase and damping velocities. The velocities increase as the value of heterogeneity parameter increases. Similar results are found regardless of the stress-free and clamped boundary conditions.
ii. The impacts of internal friction parameter of viscoelastic layer are quite interesting. The phase and damping velocities of Love waves decrease with an increase in the internal friction parameter, regardless of the stress-free and clamped boundary conditions.
iii. Effects of layer thickness on phase and damping velocities of Love waves are also demonstrated. It is noticed that phase and damping velocities decrease as the thickness of the layer increases.
iv. The impacts of imperfectness parameter G on the phase and damping velocities of Love waves are also observed. As the value of imperfectness parameter G increases, the interface becomes more perfect, meaning the bonding between the two media strengthens, resulting in an increase in phase and damping velocities. The velocities reach a maximum when the layer and half-space are perfectly bonded $G \to \infty$.

The problem covers two major aspects, first the study of Love waves, when top surface of layer is clamped, secondly the role of imperfectness that measures the bonding nature between layer and substrate on the propagation of Love waves. The findings of this paper can be useful for various areas involving applications of Love waves.

Appendix 1

$$t_1 = m_1' + i m_2' ,\quad m_1' = r^{1/2}\cos\frac{\theta}{2} ,\quad m_2' = r^{1/2}\sin\frac{\theta}{2} ,$$

$$r = (F_1^2 + F_2^2)^{1/2} ,\quad \tan\theta = \frac{F_1}{F_2} ,\quad F_1 = k^2 - \frac{a^2}{4} - \frac{\rho_0\omega^2\mu_0}{\mu_0^2 + \omega^2\eta_0^2} ,$$

$$F_2 = -\frac{\rho_0\omega^3\eta_0}{\mu_0^2 + \omega^2\eta_0^2}$$

Appendix 2

$$W_1 = \frac{1}{2}\left(1 + \frac{G}{\mu_2 kP}\right)[\mu_0(P_1Q_3 + P_2Q_4) + \omega\eta_0(P_2Q_3 - P_1Q_4)] + P_1G ,$$

$$W_2 = \frac{1}{2}\left(1 + \frac{G}{\mu_2 kP}\right)[\mu_0(P_2Q_3 - P_1Q_4) - \omega\eta_0(P_1Q_3 + P_2Q_4)] + P_2G ,$$

$$W_3 = \frac{1}{2}\left(1 + \frac{G}{\mu_2 kP}\right)[\mu_0(P_3Q_1 - P_4Q_2) + \omega\eta_0(P_3Q_2 + P_4Q_1)] + P_3G ,$$

$$W_4 = \frac{1}{2}\left(1 + \frac{G}{\mu_2 kP}\right)[\mu_0(P_3Q_2 + P_4Q_1) - \omega\eta_0(P_3Q_1 - P_4Q_2)] + P_4G ,$$

$$P_1 = \alpha\cos\alpha H + 2m_1' + 2m_1'\sin\alpha H ,\quad P_2 = 2m_2' + 2m_2'\sin\alpha H ,$$

$$P_3 = \alpha\cos\alpha H - 2m_1' - 2m_1'\sin\alpha H ,\quad P_4 = -2m_2' - 2m_2'\sin\alpha H ,$$

$$Q_1 = \alpha + 2m_1' ,\quad Q_2 = Q_4 = 2m_2' ,\quad Q_3 = \alpha - 2m_1'$$

Appendix 3

$$W_1' = \frac{1}{2\mu_2 kP}[\mu_o(P_1Q_3 + P_2Q_4) + \omega\eta_0(P_2Q_3 - P_1Q_4)] + P_1 ,$$

$$W_2' = \frac{1}{2\mu_2 kP}[\mu_o(P_2Q_3 - P_1Q_4) - \omega\eta_0(P_1Q_3 + P_2Q_4)] + P_2 ,$$

$$W_3' = \frac{1}{2\mu_2 kP}[\mu_o(P_3Q_1 - P_4Q_2) + \omega\eta_0(P_3Q_2 + P_4Q_1)] + P_3 ,$$

$$W_4' = \frac{1}{2\mu_2 kP}[\mu_o(P_3Q_2 + P_4Q_1) - \omega\eta_0(P_3Q_1 - P_4Q_2)] + P_4$$

Appendix 4

$$X_1 = \frac{1}{2}\left(1 + \frac{G}{\mu_2 kP}\right)[\mu_0Q_3 - \omega\eta_0Q_4] + G ,$$

$$X_2 = -\frac{1}{2}\left(1 + \frac{G}{\mu_2 kP}\right)[\mu_0Q_4 - \omega\eta_0Q_3] ,$$

$$X_3 = \frac{1}{2}\left(1 + \frac{G}{\mu_2 kP}\right)[\mu_0Q_1 + \omega\eta_0Q_2] + G ,$$

$$X_4 = \frac{1}{2}\left(1 + \frac{G}{\mu_2 kP}\right)[\mu_0Q_2 - \omega\eta_0Q_1]$$

Appendix 5

$$X_1' = -\frac{1}{2\mu_2 kP}[\mu_0Q_3 - \omega\eta_0Q_4] + 1 ,$$

$$X_2' = -\frac{1}{2\mu_2 kP}[\mu_0Q_4 + \omega\eta_0Q_3] ,$$

$$X_3' = \frac{1}{2\mu_2 kP}[\mu_0Q_1 + \omega\eta_0Q_2] + 1 ,$$

$$X_4' = \frac{1}{2\mu_2 kP}[\mu_0Q_2 - \omega\eta_0Q_1]$$

REFERENCES

1. Vardoulakis, I., Georgiadis, H.G. (1997), *SH surface waves in a homogeneous gradient-elastic half-space with surface energy*, J Elast. 47: 147-165. doi: 10.1023/A:1007433510623
2. Qian, Z., Jin, F., Wang, Z., Kishimoto, K. (2004), *Love waves propagation in a piezoelectric layered structure with initial stresses*, Acta Mech. 171: 41-57. doi: 10.1007/s00707-004-0128-8
3. Nakamura, K. (2007), *Shear-horizontal piezoelectric surface acoustic waves*, Jpn. J Appl. Phys. 46(7S): 4421. doi: 10.1143/JJAP.46.4421
4. Liu, Q., Zhao, M., Zhang, C. (2014), *Antiplane scattering of SH waves by a circular cavity in an exponentially graded half space*, Int. J Eng. Sci. 78: 61-72. doi: 10.1016/j.ijengsci.2014.0 2.006
5. Sharma, V., Kumar, S. (2016), *Influence of microstructure, heterogeneity and internal friction on SH waves propagation in a viscoelastic layer overlying a couple stress substrate*, Sruct. Eng. Mech. 57(4): 703-716. doi: 10.12989/sem.2016.57.4.703
6. Di Michele, F., Styahar, A., Pera, D., et al. (2022), *Fault shape effect on SH waves using finite element method*, J Seismol. 26(3): 417-437. doi: 10.1007/s10950-022-10075-y
7. Deep, S., Sharma, V. (2023), *Effects of microstructures, heterogeneity, and imperfectness on propagation of SH-waves in a fiber-reinforced layer sandwiched between two microstructural half-spaces*, Iran. J Sci. Technol. Trans. Mech. Eng. 47(3): 1161-1176. doi: 10.1007/s40997-022-00570-5

8. Drafts, B. (2001), *Acoustic wave technology sensors*, IEEE Trans. Microw. Theory Tech. 49(4): 795-802. doi: 10.1109/22.915466
9. Josse, F., Bender, F., Cernosek, R.W. (2001), *Guided shear horizontal surface acoustic wave sensors for chemical and biochemical detection in liquids*, Anal. Chem. 73(24): 5937-5944. doi: 10.1021/ac010859e
10. Ma, Q., Jiao, J., Hu, P., et al. (2014), *Excitation and detection of shear horizontal waves with electromagnetic acoustic transducers for nondestructive testing of plates*, Chin. J Mech. Eng. 27(2): 428-436. doi: 10.3901/CJME.2014.02.428
11. Ten, S.T., Hashim, U., Gopinath, S.C.B., et al. (2017), *Highly sensitive Escherichia coli shear horizontal surface acoustic wave biosensor with silicon dioxide nanostructures*, Biosens. Bioelectron. 93: 146-154. doi: 10.1016/j.bios.2016.09.035
12. Miao, H., Li, F. (2021), *Shear horizontal wave transducers for structural health monitoring and nondestructive testing: A review*, Ultrasonics, 114: 106355. doi: 10.1016/j.ultras.2021.106355
13. Deresiewicz, H. (1962), *A note on Love waves in a homogeneous crust overlying an inhomogeneous substratum*, Bull. Seismol. Soc. Am. 52(3): 639-645. doi: 10.1785/BSSA0520030639
14. Abd-Alla, A.M., Ahmed, S.M. (1999), *Propagation of Love waves in a non-homogeneous orthotropic elastic layer under initial stress overlying semi-infinite medium*, Appl. Math. Comput. 106(2-3): 265-275. doi: 10.1016/S0096-3003(98)10128-5
15. Červený, V. (2004), *Inhomogeneous harmonic plane waves in viscoelastic anisotropic media*, Studia Geophys. et Geod. 48: 167-186. doi: 10.1023/B:SGEG.0000015590.17664.70
16. Ke, L.-L., Wang, Y.-S., Zhang, Z.-M. (2005), *Propagation of Love waves in an inhomogeneous fluid saturated porous layered half-space with properties varying exponentially*, J Eng. Mech. 131(12): 1322-1328. doi: 10.1061/(ASCE)0733-9399(2005)131:12(1322)
17. Kakar, R., Kakar, S. (2018), *The torsional surface wave in a prestressed anisotropic intermediate poroelastic layer of varying heterogeneities*, J Vib. Control, 24(9): 1687-1706. doi: 10.1177/1077546316668060
18. Das, T.K., Sengupta, P.R., Debnath, L. (1991), *Thermo-viscoelastic Rayleigh waves under the influence of couple-stress and gravity*, Int. J Math. Math. Sci. 14(3): 553-560. doi: 10.1155/S0161171291000753
19. Singh, J., Singh, B., Ailawalia, P. (2011), *Propagation of waves at an imperfectly bonded interface between two monoclinic thermoelastic half-spaces*, J Theor. Appl. Mech. Sofia, 41(3): 77-92.
20. Cui, J., Du, J., Wang, J. (2013), *Study on SH waves in piezoelectric structure with an imperfectly bonded viscoelastic layer*, In: 2013 IEEE Int. Ultrasonics Symp., Prague, Czech Republic, 2013, pp.1017-1020. doi: 10.1109/ULTSYM.2013.0261
21. Singh, A.K., Parween, Z., Chatterjee, M., Chattopadhyay, A. (2015), *Love-type wave propagation in a pre-stressed viscoelastic medium influenced by smooth moving punch*, Waves Rand. Compl. Med. 25(2): 268-285. doi: 10.1080/17455030.2015.1015182
22. Chen, W.Q., Cai, J.B., Ye, G.R., Wang, Y.F. (2004), *Exact three-dimensional solutions of laminated orthotropic piezoelectric rectangular plates featuring interlaminar bonding imperfections modeled by a general spring layer*, Int. J Solids Struct. 41(18-19): 5247-5263. doi: 10.1016/j.ijsolstr.2004.03.010
23. Singh, S.S. (2011), *Love wave at a layer medium bounded by irregular boundary surfaces*, J Vib. Control, 17(5): 789-795. doi: 10.1177/1077546309351301
24. Kumar, R., Chawla, V. (2011), *Wave propagation at the imperfect boundary between transversely isotropic thermodiffusive elastic layer and half-space*. J Eng. Phys. Thermophys. 84(5): 1192-1200.
25. Li, L., Wei, P.J., Guo, X. (2016), *Rayleigh wave on the half-space with a gradient piezoelectric layer and imperfect interface*, Appl. Math. Model. 40(19-20): 8326-8337. doi: 10.1016/j.apm.2016.03.034
26. Goyal, R., Kumar, S. (2019), *Dispersion of Love waves in size-dependent substrate containing finite piezoelectric and viscoelastic layers*, Int. J Mech. Mater. Des. 15: 767-790. doi: 10.1007/s10999-019-09441-5
27. Deep, S., Goyal, R., Sharma, V. (2022), *Dispersion of Rayleigh waves in an elastic layer imperfectly attached to a microcontinuum substrate*, Mech. Solids, 57(4): 870-882. doi: 10.3103/S0025654422040069
28. Kaplunov, J., Prikazchikov, D., Sultanova, L. (2019), *Rayleigh-type waves on a coated elastic half-space with a clamped surface*, Philos. Trans. Royal Soc. A, 377(2156): 20190111. doi: 10.1098/rsta.2019.0111
29. Deep, S., Sharma, V. (2022), *Dispersion of Love waves in a dry sandy layer imperfectly attached to a microcontinuum substrate: An analysis with stress-free and clamped top surface conditions*, In: Tadepalli, T., Narayanamurthy, V. (Eds.), Recent Advances in Applied Mechanics, Lecture Notes in Mech. Eng. Springer, Singapore, pp.697-710. doi: 10.1007/978-981-16-9539-1_52.
30. Kumar, S., Sharma, V. (2024), *Influence of diverse boundary conditions on SH and P-SV wave dynamics in micropolar plates*, Thin-Wall. Struct. 198: 111708. doi: 10.1016/j.tws.2024.111708
31. Ravindra, R. (1968), *Usual assumptions in the treatment of wave propagation in heterogeneous elastic media*, Pure Appl. Geophys. 70: 12-17. doi: 10.1007/BF00875135
32. Gubbins, D., Seismology and Plate Tectonics, Cambridge University Press, 1990. ISBN 10: 0521379954